10.1098/rspa.2002.1066

Composite angle ply laminates and netting analysis

By J. T. Evans and A. G. Gibson

School of Mechanical and Systems Engineering,
University of Newcastle upon Tyne,
Newcastle upon Tyne NE1 7RU, UK
(j.t.evans@ncl.ac.uk)

Received 17 December 2001; revised 29 July 2002; accepted 21 August 2002

This paper relates to the 'netting-analysis' approach, often used in calculations of the behaviour of helically wound reinforced pressure vessels and tubes. Numerical calculation of the stress–strain relations for angle ply composite laminates often gives the impression of unexpected instability in the underlying equations. For instance, when the in-plane principal stresses are in the ratio 2:1 and the fibres are inclined at an angle close to $\theta \approx \pm \arctan \sqrt{2}$, the stress–strain relations are very sensitive to the value of θ and to the relative stiffness of the fibres and matrix. There is a simple explanation for this, which is most clearly understood by developing analytical approximations for the stress–strain relations. It is shown that the stable angle of inclination of the fibres, where no strain-induced fibre rotations occur, deviates from the so-called 'ideal' fibre angle predicted by netting analysis by an amount that depends on the matrix-to-reinforcement-stiffness ratio. When the initial angle of inclination of the fibres deviates from the stable angle, the application of strain produces fibre rotation and nonlinear stress–strain relations result. Analytical expressions for the stress–strain relations have been obtained; they show the interaction of the parameters that control the shape of the stress–strain curves.

Keywords: angle ply laminates; nonlinear stress–strain relations; netting analysis; thermoplastic matrix composites

1. Introduction

This paper relates to the behaviour of all types of tube reinforced by helically wound strengthening members. This would include, for example, fibre and wire-reinforced polymeric pipe, where the matrix is a thermoplastic, thermosetting or elastomeric polymer. The paper discusses an apparent paradox that arises when the results of 'netting analysis' (which ignores the effect of the matrix material) are compared with the full predictions of laminate theory.

When the deformation of an angle ply composite laminate is calculated using matrix methods, a common observation is the unexpected sensitivity of the results to the input data, most prominently affecting the ratio of the principal strains. For instance, with a ratio of the principal in-plane applied stresses of 2:1, it is often assumed that the ideal angle of inclination of the fibres is $\pm \arctan \sqrt{2}$, as indicated

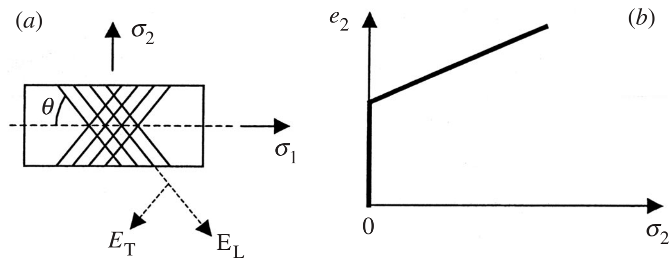

Figure 1. (*a*) Fibre orientation and applied stress. (*b*) Schematic of the stress–strain relation according to netting analysis when the fibres are not initially inclined at the ideal angle $\theta_N = \pm \arctan\sqrt{2}$. The fibres rotate at infinitesimal stress with increasing strain until they are inclined at θ_N.

by 'netting analysis'. However, experience shows that relatively small variations in the input data can produce large variations in the stress–strain relations, enough to give the impression of instability in the equations. There is a simple explanation for this, which can be most clearly demonstrated by developing approximate analytical expressions for the stress–strain relations. These reveal the interaction of the basic parameters determining the stiffness of the laminate. Such an explanation is of interest at the present time because of the need to understand the behaviour of fibre composites with matrices that show pronounced nonlinear or time-dependent mechanical behaviour. Thermoplastic matrix composites, for instance, possess a number of advantages over those with thermosetting matrices, but they can exhibit extreme differences between the stiffness of fibres and matrix in which the apparent instability becomes prominent.

2. Netting analysis

Netting analysis of the deformation of a balanced angle ply laminate gives a very simple result by ignoring the presence of the matrix and considering only the loading of the fibres (see, for example, Hull 1981; Rogers 1984), i.e. the stiffness of the matrix is taken to be effectively zero. Thus, for any given biaxial stress, there is just one critical angle of inclination of the fibres at which the laminate can support stress. In a well-known example, a reinforced rubber hose usually contains wires or fibres wound at an angle $\theta_N = \pm \arctan\sqrt{2}$ with respect to the axis of the hose. Since internal pressure produces a hoop-to-axial-stress ratio of 2:1, reinforcement at this angle would ideally support the stress in the wall material. According to the predictions of netting analysis, the two principal strains will be equal, given by

$$e_1 = e_2 = \frac{3}{2}\frac{\sigma_2}{E_L} \quad (\sigma_2 = 2\sigma_1), \tag{2.1}$$

where E_L is Young's modulus of the material in the direction of the fibres and σ_2 is the stress parallel to e_2.

If the initial angle of inclination of the reinforcement θ_i was different to θ_N, no stress could be supported. Of course, in this situation, the fibres would rotate until they reached the angle where they could support stress. The sequence of events envisaged is illustrated in figure 1. If, for the sake of argument, the initial angle of inclination θ_i was less than θ_N, the strain would initially increase under an infinitesimally small stress. In other words, the material would have zero effective stiffness. However, the resulting strain would cause the reinforcement to rotate to a new angle θ, according to the relation

$$\tan\theta = \tan\theta_{\mathrm{i}}\left(\frac{1+e_2}{1+e_1}\right), \tag{2.2}$$

where e_1 and e_2 are the principal strains in the plane of the laminate. Rotation of the fibres would thus proceed until the angle $\theta = \theta_{\mathrm{N}}$ was achieved. Taking this to be a new reference state ($\theta = \theta_{\mathrm{i}} = \theta_{\mathrm{N}}$ in (2.2)), the fibres can begin to support a finite applied stress and the material would then have finite stiffness determined by the stiffness of the fibres (figure 1). Because the two strain components would now be equal (see equation 2.1), no further rotation of the reinforcement would occur. Thus the angle θ_{N} is also the angle of stability θ_{S} in netting analysis.

Netting analysis is sometimes used to model the behaviour of laminates. However, the approximation is only likely to be accurate when the stiffness of the matrix is very small relative to that of the reinforcement. This could arise, for instance, in the case of a rubber hose and, more recently, thermoplastic matrix composites (Chapman *et al.* 1997; Chapman 1999; Gibson *et al.* 2000). In the latter materials, the matrix flows easily at relatively small strains and the effective tangent modulus of the matrix within the composite will become progressively smaller as the strain increases. One might expect that the behaviour of such a composite would approach that predicted by netting analysis at higher strains, i.e. the stiffness for both e_1 and e_2 should approach $\frac{2}{3}E_{\mathrm{L}}$. However, it is worth considering the effect of matrix stiffness, even if it is small, on the stiffness of a laminate.

Approximate analytical expressions for a balanced angle ply laminate are developed below. Here, the modulus of a lamina in the fibre direction is taken to be E_{L} and the modulus in the transverse direction is E_{T}. It is shown that the stable fibre angle θ_{S}, at which no fibre rotation accompanies increasing strain, becomes equal to the netting-analysis angle θ_{N} (equal to $\pm\arctan\sqrt{2}$) only in the limit when $E_{\mathrm{T}}/E_{\mathrm{L}} \to 0$. As in the schematic in figure 1, it is envisaged that fibres rotate with increasing strain until they are inclined at the stable angle θ_{S}. Even when the material components themselves behave elastically, fibre rotation produces nonlinear stress strain relations. Analytical expressions for the stress–strain relations, including fibre rotations, will be derived, and it will be shown that nonlinearity is controlled mainly by the deviation of the initial fibre angle θ_{i} from the stable angle θ_{S}.

3. Approximations from laminate theory

Consider an angle ply laminate loaded with biaxial stress in the ratio $\sigma_2/\sigma_1 = 2$. The material components are considered to be linear elastic. Since the arrangement has orthotropic elastic properties, the elastic constants of a lamina can be characterized by the matrix $\boldsymbol{q}$, referred to the principal axes of either one of the two reinforcements, where

$$\boldsymbol{q} = \begin{bmatrix} q_{11} & q_{12} & 0 \\ q_{12} & q_{22} & 0 \\ 0 & 0 & q_{66} \end{bmatrix} = \begin{bmatrix} E'_{\mathrm{L}} & \nu_{\mathrm{LT}}E'_{\mathrm{T}} & 0 \\ \nu_{\mathrm{LT}}E'_{\mathrm{T}} & E'_{\mathrm{T}} & 0 \\ 0 & 0 & G_{\mathrm{LT}} \end{bmatrix}. \tag{3.1}$$

Here, $E'_{\mathrm{L}} = E_{\mathrm{L}}/(1-\nu_{\mathrm{LT}}\nu_{\mathrm{TL}})$ and $E'_{\mathrm{T}} = E_{\mathrm{T}}/(1-\nu_{\mathrm{LT}}\nu_{\mathrm{TL}})$, G_{LT} is the in-plane shear modulus and ν_{LT} and ν_{TL} are the in-plane Poisson ratios. Note that $\nu_{\mathrm{TL}} = \nu_{\mathrm{LT}}E_{\mathrm{T}}/E_{\mathrm{L}}$; E_{L} and E_{T} are defined above.

The elastic constants $\boldsymbol{Q}$ for a balanced ply laminate are given by the transformed stiffness (see, for example, Hull 1981; Lekhnitskii 1963). The stress $\boldsymbol{\sigma}$ and strain $\boldsymbol{e}$ with respect to the x_1 and x_2 reference axes (figure 1) are then related by $\boldsymbol{\sigma} = \boldsymbol{Qe}$. However, by symmetry, the elastic properties of a balanced laminate also have to be orthotropic. This is achieved by assuming a constant through-thickness strain and averaging the stress through the thickness. In arriving at explicit expressions for the components of $\boldsymbol{Q}$ for a balanced angle ply laminate, the matrix in (3.1) is transformed by rotating the reference axes through $\pm\theta$. Imposition of orthotropic elastic symmetry eliminates the coupling between direct stress and shear strain. The non-zero components of $\boldsymbol{Q}$ are

$$\left.\begin{aligned}
Q_{11} &= q_{11}\cos^4\theta + 2(q_{12}+2q_{66})\sin^2\theta\cos^2\theta + q_{22}\sin^4\theta,\\
Q_{22} &= q_{11}\sin^4\theta + 2(q_{12}+2q_{66})\sin^2\theta\cos^2\theta + q_{22}\cos^4\theta,\\
Q_{12} &= q_{12}(\sin^4\theta+\cos^2\theta) + (q_{11}+q_{22}-4q_{66})\sin^2\theta\cos^2\theta,\\
Q_{66} &= (q_{11}+q_{22}-2q_{12}-2q_{66})\sin^2\theta\cos^2\theta + q_{66}(\sin^4\theta+\cos^4\theta),
\end{aligned}\right\} \tag{3.2}$$

where θ is the magnitude of the angle between the x_1-axis and the fibre directions. If the in-plane principal stress ratio σ_2/σ_1 is set to the value 2 and θ is assigned a value close to $\arctan\sqrt{2}$, numerical solutions are found to be very sensitive to the relative values of the input parameters E_{L}, E_{T}, G_{LT}, ν_{LT} and θ, to an extent that suggests instability in the equation. For this reason, it is desirable to have an analytical solution so that the interaction of the input parameters can be inspected.

In the present case, with $\sigma_2 = 2\sigma_1$, we have

$$e_1 = \sigma\frac{\frac{1}{2}Q_{22}-Q_{12}}{Q_{11}Q_{22}-Q_{12}^2}, \qquad e_2 = \sigma\frac{Q_{11}-\frac{1}{2}Q_{12}}{Q_{11}Q_{22}-Q_{12}^2}, \tag{3.3}$$

where $\sigma = \sigma_2$. Components of $\boldsymbol{Q}$ given in (3.2) can be substituted into (3.3) to obtain analytical expressions for the strain. Clearly, the result is cumbersome unless simplifications are made. We now develop approximate analytical stress–strain relations on the assumption that the stiffness of the matrix material is significantly less than that of the fibres. The connection between the elastic constants in (3.1) and the properties of the fibres and matrix are given in the various mixture rules that have been developed (see, for example, Hull 1981). These are not discussed here, but we note that as the ratio of matrix to fibre stiffness tends to zero, $E_{\mathrm{T}}/E_{\mathrm{L}} \to 0$ and $G_{\mathrm{LT}}/E_{\mathrm{L}} \to 0$, while the limiting value of E_{L} is the product of the volume fraction and Young's modulus of the fibres. In terms of the individual elastic constants in (3.1) and (3.2), this means that q_{12}, q_{22} and q_{66}, q_{12}, q_{22} and q_{66} are all much smaller than q_{11}. Thus we assume that second-order terms can be ignored. These are q_{22}^2, $q_{12}q_{22}$, $q_{12}q_{66}$ or any similar products where the subscript 2 or 6 appear twice or more in combination. It will also be assumed that the initial angle of inclination of the fibres is close to, but deviates slightly from, the ideal angle of netting analysis, i.e.

$$\theta_{\mathrm{i}} = \theta_{\mathrm{N}} + \Delta\theta. \tag{3.4}$$

Equations (3.4) and (3.2) are substituted into (3.3) together with the expressions for q in (3.1) and taking $\theta_{\mathrm{N}} = \arctan\sqrt{2}$. For concision, the symbols G_{LT} and ν_{LT} are replaced by G and ν, respectively. After some manipulation, the following expressions

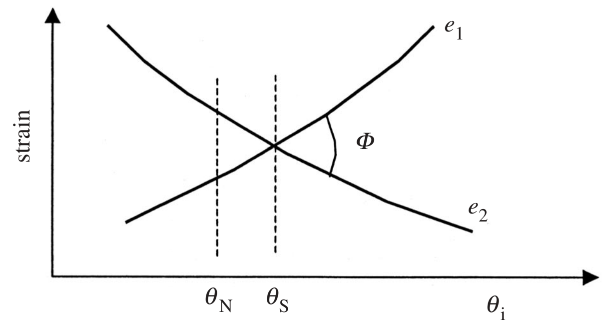

Figure 2. Relation between strain components and θ_i. In a laminate, the stable angle of inclination θ_S is not equal to θ_N.

for the strain components are obtained:

$$\left.\begin{aligned} e_1 &= \frac{3}{2}\frac{\sigma}{E_L}\frac{8G-(1+2\nu)E_T}{8G+E_T} + \frac{6\sqrt{2}\sigma}{8G+E_T}\Delta\theta, \\ e_2 &= \frac{3}{2}\frac{\sigma}{E_L}\frac{8G+(2+\nu)E_T}{8G+E_T} - \frac{3\sqrt{2}\sigma}{8G+E_T}\Delta\theta. \end{aligned}\right\} \tag{3.5}$$

Contrary to what is often believed (Rogers 1984), the stable angle for the laminate does not occur at $\theta_i = \theta_N$ ($\Delta\theta = 0$). To find the stable angle θ_S, e_1 and e_2 in (3.5) are equated to obtain

$$\theta_S = \theta_N + \frac{E_T}{E_L}\frac{(1+\nu)}{2\sqrt{2}}. \tag{3.6}$$

At this angle (figure 2), the strains become identical to those predicted by netting analysis, i.e.

$$e_1 = e_2 = \frac{3}{2}\frac{\sigma}{E_L}, \qquad \theta = \theta_S, \qquad \sigma_2 = 2\sigma_1. \tag{3.7}$$

Thus the simple approach of netting analysis gives the correct result for stiffness, but the ideal angle for support of the applied load differs from θ_N and is not simply determined by the stress ratio.

4. Comparison with laminate theory

Equations (3.5) to (3.7) hold strictly only when the ratios E_T/E_L and G/E_L become very small. The accuracy of the approximate expressions for small values can be tested against computations using the full expressions (3.2) and (3.3). The approximations in (3.5) and (3.7) are found to be reasonably accurate over a wide range of conditions.

Figure 3 shows the prediction of θ_S derived from (3.6) compared with the full numerical computation of the stable angle. As anticipated, the results converge as E_T/E_L tends to zero. When $E_T/E_L = 0.1$, the error in (3.6) is *ca.* 12%.

The predicted strain at the stable angle is given by (3.7), which does not contain the term E_T. In fact, the computed values of e_1 and e_2 are slightly dependent on E_T, as shown in figure 4. As $E_T/E_L \to 0$, the computed values of both strain components converge to $3\sigma/2E_L$. When $E_T/E_L = 0.1$, the error in the approximate expression

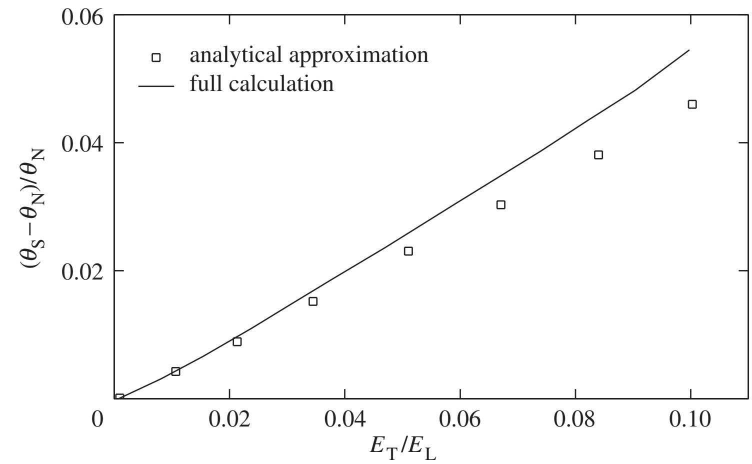

Figure 3. Deviation of the laminate stable angle from θ_N as a function of E_T/E_L. The analytical approximation is given in (3.5).

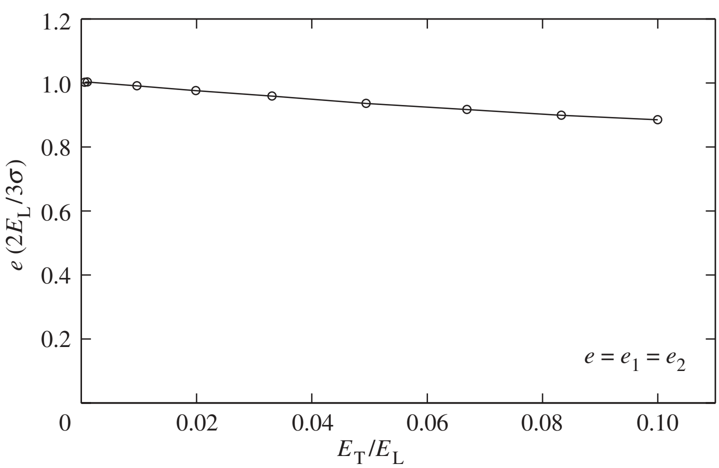

Figure 4. Strain at the stable angle as a function of E_T/E_L.

in (3.7) is 17%. For comparison, we note that the ratio E_T/E_L for glass fibre/epoxy resin plies is of the order of 0.2, for aramid/epoxy it is *ca.* 0.08 and for carbon/epoxy it is *ca.* 0.03.

Deviation of θ_i from the stable angle θ_S can have a large effect in reducing stiffness, particularly at low values of the ratio E_T/E_L. One way of quantifying this is to specify the size of the included angle Φ in the strain (e_1 and e_2) versus the θ_i relationship shown schematically in figure 2. From (3.5), it can be seen that

$$\Phi = \frac{\sigma}{E_T}\frac{9\sqrt{2}}{1 + 8G/E_T}. \tag{4.1}$$

The value of Φ indicates the extent of the reduction in stiffness when θ_i deviates from the stable angle, θ_S, by a given amount. Clearly, this is primarily dependent on the ratio σ/E_T, but the ratio of shear to transverse modulus also has an effect.

For instance, a change in the ratio G/E_{T} by a factor of three produces an order of magnitude change in Φ.

5. Rotation of fibres

The behaviour illustrated schematically in figure 1, based on netting analysis, must have its counterpart in the deformation of a laminate. This can be included by taking account of the effect of fibre rotation in calculating the strain. The analysis is aided by the following approximation obtained from (2.2),

$$\delta\theta = \tfrac{1}{2}\sin 2\theta_{\mathrm{i}}(e_2 - e_1), \tag{5.1}$$

where $\delta\theta$ is the change in the inclination of the fibres produced by the strain and θ_{i} is the initial inclination at zero strain. The strain-dependent deviation from the ideal netting angle is equal to $(\theta_{\mathrm{i}} - \theta_{\mathrm{N}}) + \frac{1}{2}\sin 2\theta_{\mathrm{i}}(e_2 - e_1)$. Thus (3.5) can be rewritten as

$$\left.\begin{aligned} e_1 &= \frac{3}{2}\frac{\sigma}{E_{\mathrm{L}}}\frac{8G-(1+2\nu)E_{\mathrm{T}}}{8G+E_{\mathrm{T}}} + \frac{6\sqrt{2}\sigma}{8G+E_{\mathrm{T}}}[(\theta_{\mathrm{i}}-\theta_{\mathrm{N}}) + \tfrac{1}{2}\sin 2\theta_{\mathrm{i}}(e_2-e_1)],\\ e_2 &= \frac{3}{2}\frac{\sigma}{E_{\mathrm{L}}}\frac{8G+(2+\nu)E_{\mathrm{T}}}{8G+E_{\mathrm{T}}} - \frac{3\sqrt{2}\sigma}{8G+E_{\mathrm{T}}}[(\theta_{\mathrm{i}}-\theta_{\mathrm{N}}) + \tfrac{1}{2}\sin 2\theta_{\mathrm{i}}(e_2-e_1)]. \end{aligned}\right\} \tag{5.2}$$

Solving (5.2) and rearranging gives expressions for strain, including fibre rotation. After some manipulation, we obtain

$$\left.\begin{aligned} e_1 &= \frac{3}{2}\frac{\sigma}{E_{\mathrm{L}}}\left[1 - \frac{2(1+\nu)E_{\mathrm{T}} - 4\sqrt{2}E_{\mathrm{L}}(\theta_{\mathrm{i}}-\theta_{\mathrm{N}})}{8G+E_{\mathrm{T}}+(9/\sqrt{2})\sin 2\theta_{\mathrm{i}}\sigma}\right],\\ e_2 &= \frac{3}{2}\frac{\sigma}{E_{\mathrm{L}}}\left[1 + \frac{(1+\nu)E_{\mathrm{T}} - 2\sqrt{2}E_{\mathrm{L}}(\theta_{\mathrm{i}}-\theta_{\mathrm{N}})}{8G+E_{\mathrm{T}}+(9/\sqrt{2})\sin 2\theta_{\mathrm{i}}\sigma}\right]. \end{aligned}\right\} \tag{5.3}$$

Interpretation of the effect of parameters in (5.3) is aided by noting the value of the angle of stability given by (3.6). As a result, equation (5.3) can be recast in the form

$$\left.\begin{aligned} e_1 &= \frac{3}{2}\frac{\sigma}{E_{\mathrm{L}}}\left[1 - \frac{4\sqrt{2}E_{\mathrm{L}}(\theta_{\mathrm{S}}-\theta_{\mathrm{i}})}{8G+E_{\mathrm{T}}+(9/\sqrt{2})\sin 2\theta_{\mathrm{i}}\sigma}\right],\\ e_2 &= \frac{3}{2}\frac{\sigma}{E_{\mathrm{L}}}\left[1 + \frac{2\sqrt{2}E_{\mathrm{L}}(\theta_{\mathrm{S}}-\theta_{\mathrm{i}})}{8G+E_{\mathrm{T}}+(9/\sqrt{2})\sin 2\theta_{\mathrm{i}}\sigma}\right]. \end{aligned}\right\} \tag{5.4}$$

It is clear that the deviation of the initial fibre angle from the stable angle has a major influence on the nonlinearity in the stress–strain relations. When $\theta_{\mathrm{i}} = \theta_{\mathrm{S}}$ in (5.4), the relations become identical to the linear stress–strain relations from netting analysis given in (3.7). Examples of the nonlinear relations obtained from (5.4) when $\theta_{\mathrm{i}} \neq \theta_{\mathrm{S}}$ are given below.

When $\theta_{\mathrm{i}} \approx \theta_{\mathrm{S}}$, the result is not too different from netting analysis. Thus the curves in figure 5 are obtained by taking $(\theta_{\mathrm{S}} - \theta_{\mathrm{i}}) = 0.001\theta_{\mathrm{N}}$ and $E_{\mathrm{T}}/G = 2$. As $E_{\mathrm{T}}/E_{\mathrm{L}}$ becomes progressively smaller, the effect of the small angular deviation becomes more pronounced.

Greater variations in the stress–strain relations occur with larger angular deviations. With $(\theta_{\mathrm{S}} - \theta_{\mathrm{i}}) = 0.01\theta_{\mathrm{N}}$, for instance, divergent stress dependencies of e_1 and

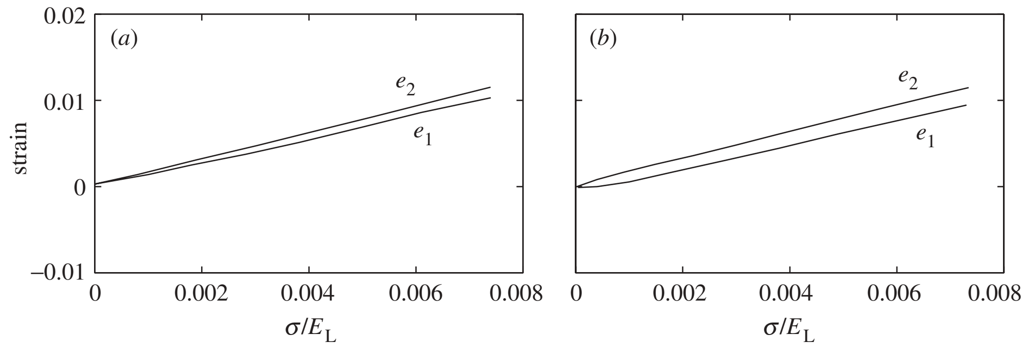

Figure 5. Effect of the ratio E_T/E_L on the stress–strain relations with a small deviation, $(\theta_S - \theta_i) = 0.001\theta_N$, of the initial fibre inclination from the stable angle. (*a*) $E_T/E_L = 10^{-2}$. (*b*) $E_T/E_L = 10^{-3}$.

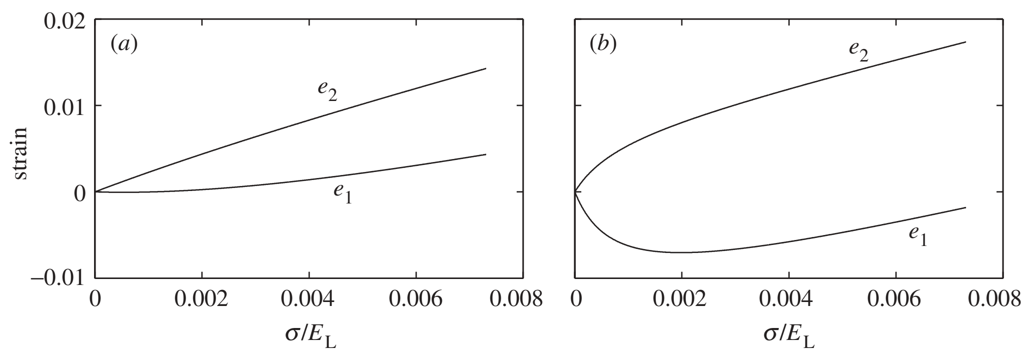

Figure 6. Effect of the ratio E_T/E_L on the stress–strain relations with a larger deviation, $(\theta_S - \theta_i) = 0.01\theta_N$, of the initial fibre inclination from the stable angle. (*a*) $E_T/E_L = 10^{-2}$. (*b*) $E_T/E_L = 10^{-3}$.

e_2 are observed, particularly with small values of E_T/E_L (figure 6). Note that the stress–strain relations in figure 6*b* are similar to those envisaged in the case of netting analysis when $\theta_i \neq \theta_N$ (figure 1). As the strain increases, however, the slopes of the curves for both strain components approach $3/(2E_L)$ asymptotically, in line with the principal result of netting analysis.

6. Discussion

This paper seeks to clarify a common observation in the calculation of the properties of angle ply laminates. With fibre angles close to the ideal netting theory angle, the results of computations based on numerical matrix methods are very sensitive to the input data. One reason for this is that the stable angle θ_S itself depends on the properties of the plies, as shown in (3.6) above. When $\theta_i = \theta_S$, the stress–strain relations are exactly equal to those given by netting analysis and depend only on the value of E_L. When $\theta_i \neq \theta_S$, the strains are given by the more complicated expressions in (3.5). These are simplified somewhat by taking $\theta_i = \theta_N$. Even so, the resulting strains are sensitive to the relative values of E_T and G. Then the netting-analysis

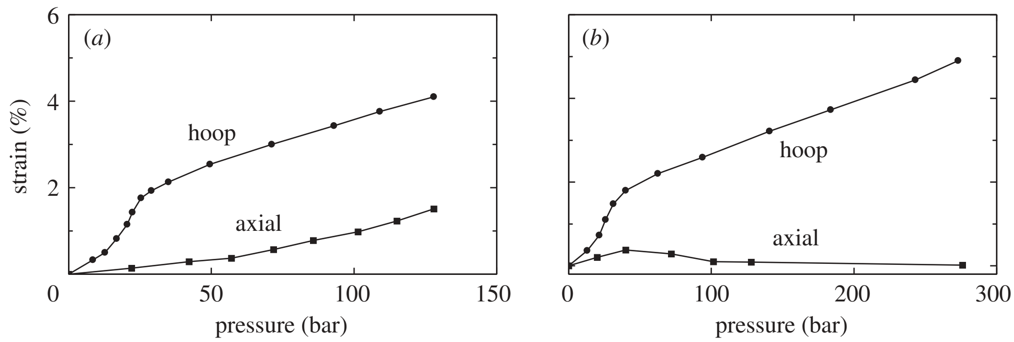

Figure 7. Examples of stain versus pressure in two thermoplastic reinforced pipes ((*a*) pipe A and (*b*) pipe B) supplied by two different manufacturers (after Chapman 1999).

stress–strain relations (2.2) are only recovered when the ratio E_T/G is made equal to zero.

A full picture of deformation is obtained only when strain-induced fibre rotation is incorporated. This can be done with relative simplicity using the analytic approximations shown in (3.5). The result, giving nonlinear stress–strain relations, is shown in (5.4). This includes the possibility that the fibres will rotate with increasing strain until the stable angle is achieved. When this occurs, the slopes of the stress–strain curves will be equal to $\frac{2}{3}E_L$ for both e_1 and e_2. Of course, insufficient fibre rotation may have occurred at a given stress level to achieve the stable angle. This depends on the relative values of E_T and G. When the ratios E_T/E_L and G/E_L are relatively large, insufficient fibre rotation occurs to achieve the stable angle with stress values σ/E_L below, say, 0.08 (figure 6*a*). With much smaller values of E_T/E_L, fibre rotations large enough to achieve the stable angle occur at low stress values (figure 6*b*).

The above treatment of deformation assumes boundary conditions of constant biaxial stress with a constant stress ratio. This is a statically determinate applied stress field, such as is approximated in the deformation of an internally pressurized tube at points remote from the ends of the tube. These assumptions would, of course, be invalid if, instead of a constant stress ratio, a constant biaxial strain were imposed, because no fibre rotation could then occur. It follows that one would not expect the simplified model to apply to deformation near the ends of an internally pressurized tube because of the constraints on displacement of the tube at this location.

This treatment is relevant to understanding the deformation of composites comprising fibres in a matrix with much lower stiffness. Certain types of thermoplastic matrix composite could be considered to belong to this category. In reinforced polyethylene pipes, for instance, the matrix can deform extensively during pressurization (Chapman *et al*. 1997; Gibson *et al*. 2000). Nonlinear viscoelastic deformation of the matrix means that the effective stiffness of the matrix declines systematically as the pressure increases. The assumptions leading to (5.4) could then be justified for deformation at higher strains. Examples of hoop and axial strain as a function of internal pressure are shown in figure 7 for thermoplastic fibre reinforced pipes supplied by two different manufacturers (Chapman 1999). The reinforcement used was aramid fibre (Twaron®) reinforced tape. Tapes were wound over a high-density polyethylene liner at a nominal angle $\pm \arctan\sqrt{2}$ to the axis. A medium-density polyethylene external layer was added by extrusion. Pipe B contains double the amount of reinforcement as pipe A, so the properties are not directly comparable. It is not intended to compare the above model directly with the experimental results in figure 7, since nonlinear viscoelastic deformation in the matrix is more complex behaviour than is considered in the present paper and has to be modelled numerically (Chapman 1999; Gibson *et al*. 2000). Nevertheless, the results in figure 7 illustrate the variations in stress–strain behaviour that has often been observed in tests on reinforced thermoplastic pipes. The above analytical treatment gives an insight into the interaction of the key parameters and why such variations might occur in practice.

7. Conclusions

(i) It can be shown that the stable angle of inclination of the fibres, where no fibre rotation occurs with increasing strain, differs from the ideal angle of netting analysis by an amount that depends on the matrix-to-fibre-stiffness ratio.

(ii) When the initial angle of inclination of the fibres is identical to the stable angle, the stress–strain relations are the same as those given by netting analysis.

(iii) When the initial angle of inclination of the fibres differs from the stable angle, fibre rotation and nonlinear stress–strain relations result. Analytical expressions revealing the interaction of the parameters in their effect on deformation were obtained.

The results shown in figure 7 are from the PhD thesis of Dr B. J. Chapman. The authors are currently in receipt of an EPSRC ROPA award relating to 'The Manufacture of Reinforced Thermoplastic Pipes'.

References

Chapman, B. J. 1999 Continuous reinforced thermoplastic pipes. PhD thesis, University of Newcastle upon Tyne, UK.

Chapman, B. J., Evans, J. T., Frost, S. R. & Gibson, A. G. 1997 Mechanical testing of continuous fibre reinforced thermoplastic pipes. In *11th Int. Conf. on Composite Materials, Gold Coast, Australia, 14–18 July 1997* (ed. M. L. Scott), vol. V, pp. 517–526. Australian Composite Structures Society Woodhead Publishing Ltd.

Gibson, A. G., Hicks, C., Wright, P. N. H. & Fahrer, A. 2000 *Plastics Rubber Composites* **9**, 509–519.

Hull, D. 1981 *An introduction to composite materials*. Cambridge University Press.

Lekhnitskii, S. G. 1963 *Theory of elasticity of an anisoptopic body*. San Francisco, CA: Holden-Day.

Rogers, T. G. 1984 Problems for helically wound cylinders. In *Continuum theory of the mechanics of fibre-reinforced composites* (ed. A. J. M. Spencer), pp. 147–178. Springer.